

available at [www.sciencedirect.com](http://www.sciencedirect.com)journal homepage: [www.ejconline.com](http://www.ejconline.com)

# Additional value of MR/PET fusion compared with PET/CT in the detection of lymph node metastases in cervical cancer patients

Seok-Ki Kim<sup>a</sup>, Hyuck Jae Choi<sup>a,\*</sup>, Sang-Yoon Park<sup>a</sup>, Ho-Young Lee<sup>b</sup>, Sang-Soo Seo<sup>a</sup>, Chong Woo Yoo<sup>a</sup>, Dae Chul Jung<sup>a</sup>, Sokbom Kang<sup>a</sup>, Kyung-Sik Cho<sup>a</sup>

<sup>a</sup>Department of Radiology, Asan Medical Center, University of Ulsan, 388-1, Poongnap-dong, Songpa-gu, Seoul 138-736, Republic of Korea

<sup>b</sup>Department of Nuclear Medicine, Seoul Metropolitan Boramae Hospital, Boramae Road, Dongjak-Gu, Seoul 156-707, Republic of Korea

## ARTICLE INFO

### Article history:

Received 12 February 2009

Received in revised form 12 March 2009

Accepted 1 April 2009

Available online 4 May 2009

### Keywords:

Cervical cancer

Magnetic resonance imaging

Positron emission tomography

Fusion

Lymph node metastasis

## ABSTRACT

We evaluated the additional diagnostic value of magnetic resonance/positron emission tomography (MR/PET) fusion in the detection of metastatic lymph nodes in cervical cancer patients.

Seventy nine patients with FIGO stage IB-IVA cervical cancer who had undergone both magnetic resonance imaging (MRI) and positron emission tomography/computed tomography (PET/CT) before lymphadenectomy were included in this study. Image analysis was first performed with PET/CT images only. A second analysis was then performed with MR/PET fused images that focused on the additional information obtained from the MR images. Lymphadenectomy involved removing all visible lymph nodes in the surgical field. To enable nodal group-specific comparisons, para-aortic and pelvic lymph nodes were divided into seven nodal groups: para-aortic, both common iliac, both external iliac and both internal iliac/obturator areas. Histopathological evaluation of lymph nodes has been the diagnostic standard. The value of the additional information from the MR images was evaluated by means of receiver operating characteristic (ROC) analysis.

Fused MR/PET rendered readers to detect six more metastatic lymph node groups. The sensitivity and specificity of PET/CT and fused MR/PET were 44.1%, 93.9% and 54.2%, 92.7% respectively. The ROC analysis demonstrated a higher diagnostic performance of fused MR/PET compared to PET/CT alone for detecting lymph node metastases ( $p = 0.0259$ ).

The findings of this study demonstrate the additional diagnostic value of fused MR/PET images compared with PET/CT in the detection of metastatic lymph nodes in patients with uterine cervical cancer.

© 2009 Elsevier Ltd. All rights reserved.

## 1. Introduction

Cervical cancer is the second most frequently diagnosed malignancy in women worldwide, and is the only major

gynaecological malignancy clinically staged according to the International Federation of Obstetrics and Gynaecology (FIGO) recommendations.<sup>1</sup> In patients with cervical cancer, the presence of lymph node metastases is associated with a poor

\* Corresponding author. Tel.: +82 2 3010 5686; fax: +82 2 476 4719.

E-mail address: [choihj@amc.seoul.kr](mailto:choihj@amc.seoul.kr) (H.J. Choi).

0959-8049/\$ - see front matter © 2009 Elsevier Ltd. All rights reserved.

doi:10.1016/j.ejca.2009.04.006

prognosis.<sup>2–4</sup> Lymph node involvement is also an important factor for the choice of adjuvant radiotherapy.<sup>5</sup> Subsequent surgical staging shows that clinical staging of cervical cancers is accurate in only approximately 60% of cases,<sup>6,7</sup> with undiagnosed lymph node metastases being a major problem.<sup>6–8</sup> Although nodal resection before radiotherapy results in improved survival in patients with grossly enlarged pelvic and para-aortic lymph nodes,<sup>9,10</sup> routine pretreatment surgical staging is not recommended because it is specialised and increases the time and cost of procedure, with an increased risk of immediate and delayed complications in patients.<sup>11–13</sup>

Recently, positron emission tomography (PET) employing the glucose analogue [<sup>18</sup>F]-flouro-2-deoxy-D-glucose (FDG) has been shown to be more sensitive than computed tomography (CT) or magnetic resonance imaging (MRI) for detecting lymph node metastases in cervical carcinoma patients.<sup>14–19</sup> However, PET has lower spatial resolution than CT or MRI. Fused PET/CT, as described by Beyer et al., combines the anatomic detail provided by CT with PET metabolic information.<sup>20</sup> Initial studies have shown that this technique has improved the anatomical localisation of PET abnormalities and reduced the number of equivocal PET interpretations.<sup>21–24</sup> PET/CT has gradually become a popular modality for detecting metastatic lymph nodes in patients with cervical cancer. However, it has not yet been established whether PET/CT alone is the best imaging technique for examining patients with cervical cancer. Although it is difficult for radiologists to characterise small lymph nodes, we thought that it might improve patient management if small metastatic lymph nodes could be identified by fused MR/PET imaging preoperatively, because MRI is better for tissue characterisation when compared with CT (especially non-contrast CT). However, to date there has been no study on the additional usefulness of fused MR/PET imaging in detecting metastatic lymph nodes in patients with uterine cervical cancer.

Therefore, we performed this study to evaluate the diagnostic value of fused MR/PET imaging in the detection of metastatic lymph nodes in cervical cancer patients.

## 2. Patients and methods

### 2.1. Patients

This was a retrospective study and our institutional review board did not require approval or informed consent for review of patients' records or images. The inclusion criteria for patients were as follows: untreated patients with histopathologically confirmed FIGO stage IB to IVA invasive cervical cancer determined by a conventional work-up that included MR images between October 2001 and December 2007; age 29–73 years (mean = 50 years); no contraindication to the surgical procedure; no evidence of distant metastases; an Eastern Cooperative Oncology Group performance status of 0–1. Those with small cell carcinoma ( $n = 5$ ) and patients who were not to undergo laparoscopic lymph node dissection were excluded ( $n = 50$ ).

All patients were classified into two groups according to FIGO staging. The first group consisted of patients with stage IB1 (tumour size  $\leq 4$  cm) and IIA, and they received conventional lymphadenectomy combined with a radical hysterectomy

via laparotomy ( $n = 59$ ). The second group consisted of patients with stage IB2 or  $\geq$  IIB, and they received chemoradiation preceded by laparoscopic para-aortic and pelvic lymphadenectomy ( $n = 20$ ).

Informed consent was obtained from all patients in the second group before the laparoscopic para-aortic and pelvic lymphadenectomy.

### 2.2. Conventional staging work-up

After histological confirmation of invasive cervical cancer, the FIGO stage was determined using bimanual pelvic examination (P.S.Y., S.S.S.), cystoscopy and sigmoidoscopy.

### 2.3. MRI

MRI was performed with the Signa 1.5 T system (General Electric Medical Systems, Milwaukee, WI) using a pelvic array coil for the pelvic scan and a torso phase array coil for the para-aortic scan. Scans were performed using the following parameters: axial T1-weighted fast spin-echo sequence (TR/TE, 600 ms/10 ms; slice thickness, 5 mm; interslice gap, 2 mm; field of view, 24 cm  $\times$  24 cm; matrix, 256  $\times$  192; echo-train length, 4; three signals acquired; no fat saturation; bandwidth, 31.25 kHz), axial T2-weighted fast spin-echo sequence (TR/TE, 5000/68 ms; slice thickness 3 mm; interslice gap 1 mm; 24 cm  $\times$  24 cm field of view, matrix, 256  $\times$  192; echo-train length, 21; four signals acquired; no fat saturation, 31.25 kHz bandwidth), sagittal T2-weighted fast spin-echo sequence (TR/TE, 5000/68 ms; slice thickness, 3 mm; interslice gap, 3 mm; field of view, 24 cm  $\times$  24 cm; matrix, 256  $\times$  192; echo-train length, 26; four signals acquired; no fat saturation, 31.25 kHz bandwidth), coronal T2-weighted fast spin-echo sequence (TR/TE, 5000/68 ms; slice thickness, 3 mm; interslice gap, 3 mm; field of view, 24 cm  $\times$  24 cm; matrix, 256  $\times$  192; echo-train length, 26; four signals acquired; no fat saturation, 31.25 kHz bandwidth), gadolinium-enhanced axial and sagittal T1 weighted turbo spin-echo sequence (TR/TE, 175/4.2 ms; slice thickness, 5 mm; interslice gap, 2 mm; 24 cm  $\times$  24 cm field of view for axial plane and 24 cm  $\times$  24 cm field of view for sagittal plane; matrix, 256  $\times$  192; echo-train length, 3; two signals acquired; fat saturation; bandwidth, 31.25 kHz) for the pelvic region, and axial fast spin-echo T2-weighted sequence with 16 s of breath holding (TR/TE, 2000/68 ms; slice thickness, 8 mm; interslice gap 2 mm; field of view, 32 cm  $\times$  24 cm; matrix, 256  $\times$  160; echo-train length, 20; one signal acquired; no fat saturation, 31-kHz bandwidth) for the para-aortic region. Ten patients did not have a gadolinium injection because from March 2004 to October 2004 we did not obtain the gadolinium-enhanced T1-weighted MR sequences and these patients were recruited during that period of time.

### 2.4. PET/CT imaging protocol

Whole-body PET/CT was performed using either one of two combined PET/CT scanners: a Biograph LSO (Siemens Medical Solutions, Hoffman Estates, IL) or a Discovery LS (General Electric Medical Systems, Milwaukee, WI). The choice of scanner was arbitrary, with the Biograph LSO used on 43 patients

and the Discovery LS scanner used on 36 patients. PET/CT scans were carried out between 2 and 20 days (mean + SD = 7 + 6 days) before surgery.

After an 8 h fast, patients were intravenously injected with 444–740 MBq (12–20 mCi) FDG and encouraged to rest. PET/CT scanning was performed from the middle of the skull to the upper thigh 60 min after injection and an additional regional PET/CT scan was performed from the upper margin of the left kidney to the pelvic floor 120 min after injection. On each PET/CT scan, spiral CT was performed using the following parameters: for the Biograph LSO scanner, a scout view at 30 mA and 130 kVp, followed by a spiral CT scan with a 0.8 s rotation time, 50 mA, 130 kVp, 5 mm section width, 4 mm collimation, 12 mm table feed per rotation, with arms raised; for the Discovery LS scanner, a scout view at 30 mA and 120 kVp, followed by a spiral CT scan with a 0.8 s rotation time, 80 mA, 140 kVp, 5 mm section thickness, 4.25 mm interval in high-speed mode, with arms at the sides of the torso. PET image acquisition followed CT scanning (3 min per bed position of 11.2 cm in 3-dimensional acquisition mode [Biograph LSO] or 4 min per bed position of 14.2 cm in 2-dimensional acquisition mode [Discovery LS]). CT images were reconstructed onto a 512 × 512 matrix, and were converted into 511-keV-equivalent attenuation factors for attenuation correction. PET images were reconstructed onto a 128 × 128 matrix using ordered subset expectation maximisation and attenuation correction. The standardised uptake value (SUV) was calculated as follows:  $SUV = (\text{decay-corrected activity [kBq]} / \text{ml of tissue volume}) / (\text{injected } ^{18}\text{F-FDG activity [kBq]} / \text{body mass [g]})$ . The SUV of the lesion was obtained by placing regions of interest (ROI) manually around the lesion and the maximum SUV within an ROI was used to minimise partial-volume effects. PET, PET/CT and CT images were analysed using a dedicated workstation and eNtegra (General Electric Medical Systems) and e.soft (Siemens Medical Solutions) software which allowed three-dimensional image display (transaxial, coronal and sagittal) and maximum intensity projection of PET data.

## 2.5. Image fusion

Ordered subset expectation maximisation-reconstructed images of PET/CT studies were transferred in digital imaging and communication in medicine (DICOM) format to a commercially available personal-based system (Advantage Workstation, version 4.3, GE Healthcare Technology) via the intranet. MR and PET/CT images were stored in a common database and the MR images were registered to CT images of PET using a semi automatic voxel-based algorithm. After registration, the coregistered images were reconstructed and visualised in the axial planes. Alignment in all three planes was assessed by checking the body outline and the position of metabolically active motionless organs (vein, bone and spine).

## 2.6. Classification of lymph nodal groups

Para-aortic and pelvic lymph nodes were classified into seven groups according to the nearest largest artery: para-aortic (including right and left para-aortic lymph nodes), both com-

mon iliac, both external iliac and both internal iliac/obturator areas (Fig. 1).

## 2.7. Surgical technique

All patients underwent preoperative bowel preparation for 2 days, were given prophylactic antibiotics, and underwent surgery using the same instruments and techniques. Two gynaecologic surgeons (P.S.Y., S.S.S.) performed all operations. The surgeons were aware of the MRI and PET/CT findings with regard to lymph nodes prior to performing lymph node dissections. The first group (patients with stage IB1 and IIA) received conventional lymphadenectomy combined with a radical hysterectomy via laparotomy ( $n = 59$ ), while the second group (patients with stage IB2 or  $\geq$  IIB) received a laparoscopic para-aortic and pelvic lymphadenectomy ( $n = 20$ ).

For both groups, lymphadenectomy was performed systematically with sampling of all node groups. All harvested lymph nodes were grouped according to the name of the adjacent vessel (abdominal aorta, both common iliac arteries, both external iliac arteries and both internal iliac and obturator arteries). For discrimination of the external iliac lymph node group from the internal/obturator node group we

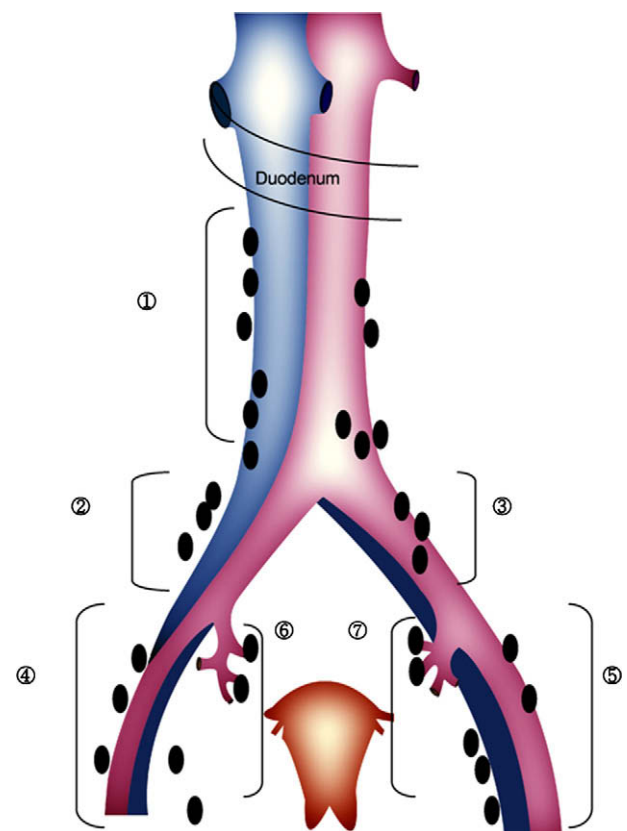


**Fig. 1 – Classification of para-aortic and pelvic lymph node groups (cited from Cancer. 2006 Feb 12;106(4):916, figure 1).** Para-aortic lymph nodes right common iliac lymph nodes left common iliac lymph nodes right external iliac lymph nodes left external iliac lymph nodes right internal iliac/obturator lymph nodes left internal iliac/obturator lymph nodes.

**Table 1 – The number of truly or falsely diagnosed patients or nodal group with PET/CT and fused MR/PET in the detection of metastatic lymph node groups in cervical cancer patients.**

|                             | PET/CT <sup>a</sup><br>Patients (number) | Fused MR/PET <sup>b</sup><br>Patients (number) | PET/CT <sup>a</sup><br>Nodal groups (number) | Fused MR/PET <sup>b</sup><br>Nodal groups (number) |
|-----------------------------|------------------------------------------|------------------------------------------------|----------------------------------------------|----------------------------------------------------|
| Total (number)              | 79                                       | 79                                             | 553                                          | 553                                                |
| True positive               | 14                                       | 17                                             | 26                                           | 32                                                 |
| True negative               | 35                                       | 33                                             | 464                                          | 456                                                |
| False positive              | 14                                       | 16                                             | 30                                           | 38                                                 |
| False negative              | 16                                       | 13                                             | 33                                           | 27                                                 |
| Total positive <sup>c</sup> | 30                                       | 30                                             | 59                                           | 59                                                 |
| Total negative <sup>d</sup> | 49                                       | 49                                             | 494                                          | 494                                                |

a Image analysis was done with PET/CT only.

b Image analysis was done with fused MR/PET.

c Total number of patients or nodal groups with pathologically confirmed metastatic lymph nodes.

d Total number of patients or nodal groups with pathologically confirmed non-metastatic lymph nodes.

classified the lymph nodes, which were located parallel or anterior to the external iliac artery, as the external iliac lymph node group, and the nodes which were located posterior to the external iliac artery and near the internal iliac or obturator artery, as the internal iliac/obturator lymph node group. The upper limit of para-aortic lymph node dissection was the duodenum, and the margin of node dissection was demarcated using endoclips and this was confirmed by abdominal X-ray after surgery.

## 2.8. Histopathological evaluation

Histopathological evaluation of lymph nodes was the diagnostic standard. Thin sections were stained with haematoxylin and eosin, and examined microscopically by a pathologist (Y.J.W.).

## 2.9. Analysis and statistics

PET/CT images were interpreted by one nuclear physician (K.S.K.) with 7 years of experience in PET imaging, and fused MR/PET images were interpreted by consensus of one radiologist (C.H.J.) with 7 years of experience in gynaecologic imaging and one nuclear physician (K.S.K.). The readers were informed of patient history in that they knew all patients had undergone systemic lymph node dissection for cervical cancer; however, the readers were blinded to the presence of metastatic lymph nodes for all patients. First, the nuclear physician reviewed the PET/CT only. Two months later, the radiologist and nuclear physician interpreted the fused MR/PET together. They focused on the additional value of MR images as a backbone for PET images in detecting metastatic lymph nodes. The images were presented in random order to each of the readers at each session. MR images were examined in the picture archiving and communication system. For PET/CT and fused MR/PET images, interpretations were made visually using a 5-point grading system: 0 = negative findings, 1 = insignificant, yet visible lesion, 2 = equivocal, needs further follow-up, 3 = probably metastasis, 4 = significant metastasis.<sup>25,26</sup> To utilise the additional information of MR, the size and border of lymph nodes were evaluated in fused MR/PET interpretation.<sup>27</sup> PET/CT and fused MR/PET images were examined directly from the

screen of a computer workstation. Information from PET/CT and fused MR/PET evaluations were entered into a prospective database; the histopathology staging information was stored in a separate file.

The value of additional MR/PET fusion was evaluated by means of receiver operating characteristic (ROC) analysis. Analysis was performed with computer software (STATA, version 9.2; Stata Corp, Texas). A *p* value of 0.05 or less was considered to indicate a significant difference.

## 3. Results

There were metastatic lymph nodes in 59 (10.7%) of 553 nodal groups in 30 (38.0%) of the 79 patients. 17 patients had one metastatic nodal group, seven had two groups and six had three to five groups.

26 (44.1%) metastatic nodal groups in 26 patients were identified on PET/CT images. After review of fused MR/PET images obtained in 79 patients, the nuclear physician and radiologist changed the visual grade level score of 30 nodal groups in 28 patients which led readers to identify six more metastatic nodal groups in three more patients and 32 (47.1%) metastatic nodal groups in 17 patients (Table 1) (Figs. 2 and 3).

The positive predictive value, negative predictive value, sensitivity, and specificity are summarised in Table 2. The area under the ROC was 0.690 (confidence interval; 0.650–0.728) for the PET/CT and 0.735 (0.696–0.771) for fused MR/PET (Fig. 4). Comparison of the areas under the ROC curves for the detection of viable tumour demonstrated a significant difference (*p* = 0.045) between the PET/CT and fused MR/PET.

## 4. Discussion

The presence of metastatic lymph nodes radically influences the prognosis and treatment of patients with cervical cancer.<sup>8–11</sup> In locally advanced cervical cancer patients, the 5-year survival rate in node-negative patients is 57%, and this is reduced to 34% when pelvic nodes are involved, and to 12% when para-aortic nodes are involved in surgically staged, locally advanced cervical cancer patients.<sup>28</sup> However, the presence of lymph node metastases does not alter the clinical



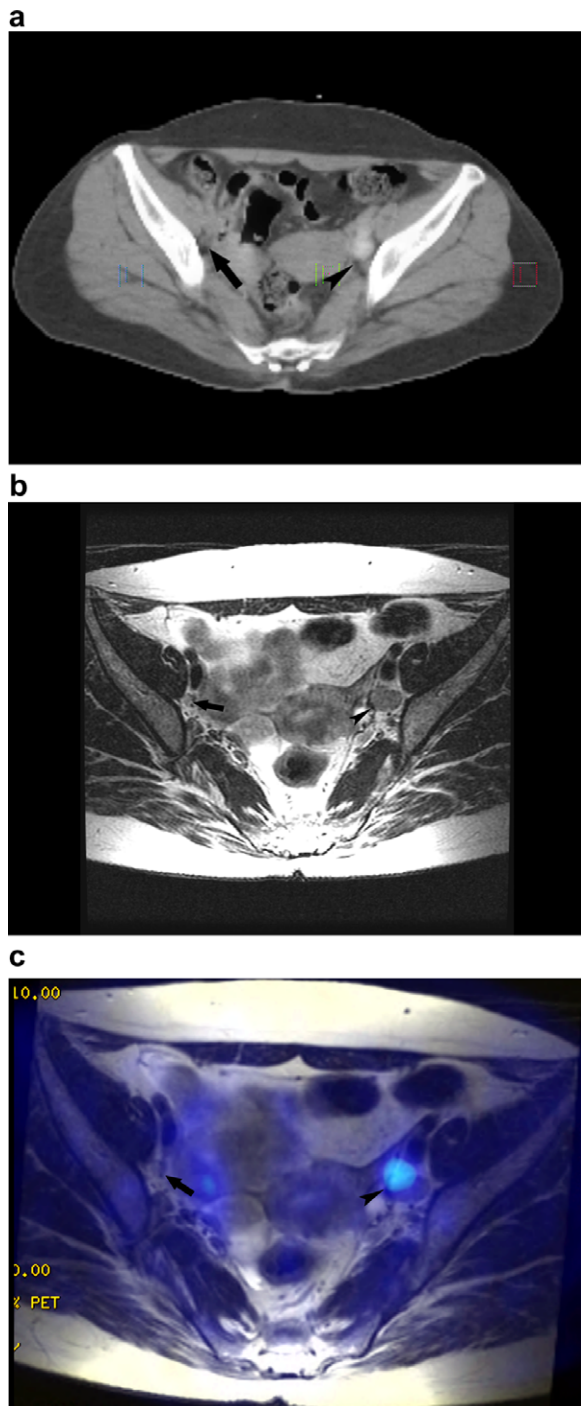


**Fig. 2** – True-positive metastasis in both internal iliac lymph nodes of a 36-year-old woman with stage IIIA uterine cervical cancer. (a) Transaxial PET/CT scan showing no abnormally high uptake (arrow) in the right internal iliac area. Note increased uptake in the left internal iliac area (arrowhead). (b) T2 weighted axial image showing lymph node (short axis diameter = 5 mm) with lobulated margin in the right internal iliac area (arrow). Note large lymph node (short axis diameter = 13 mm) in the left internal iliac area (arrowhead). (c) Fused MR/PET axial image showing no definite increased FDG uptake in the right internal iliac lymph node (arrow). Note increased uptake in the left internal iliac lymph node (arrowhead).

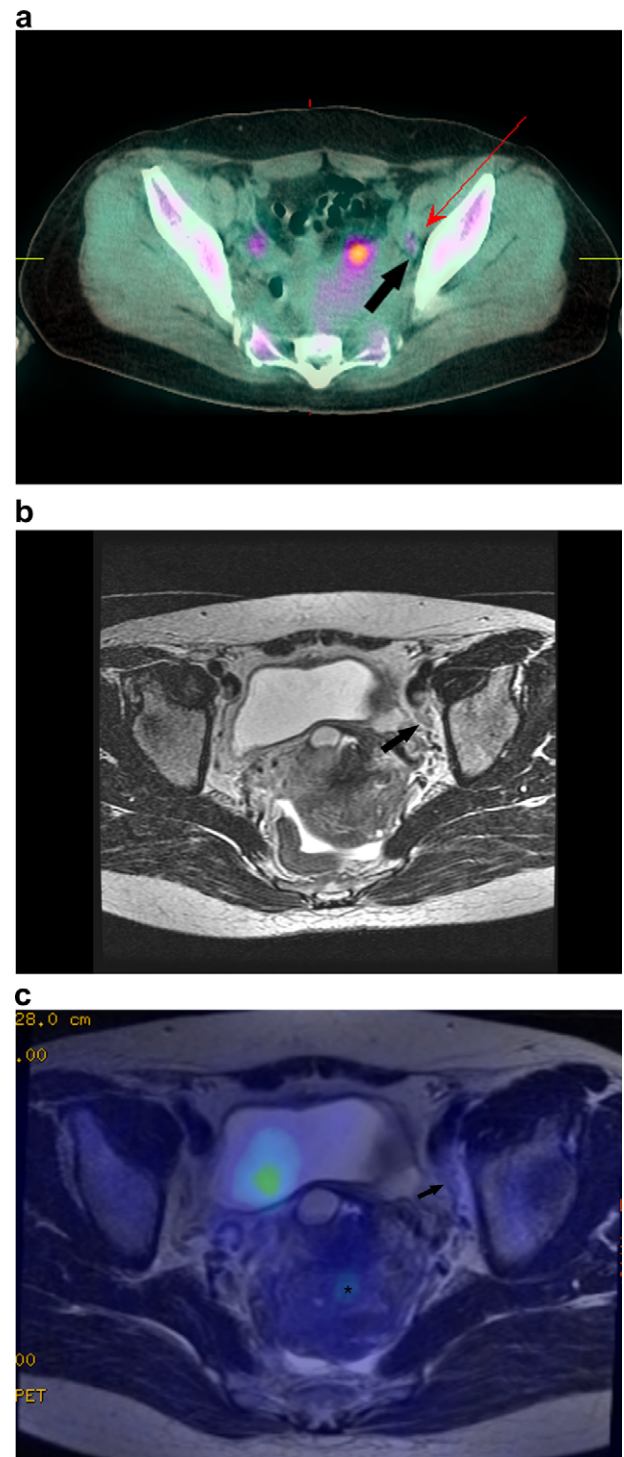


**Fig. 3** – True-positive metastasis in the left internal iliac lymph node of a 47-year-old woman with stage IIB uterine cervical cancer. (a) Transaxial PET/CT scan showing slightly increased uptake in the left internal iliac area (arrow). (b) T2 weighted axial image showing lymph node (short axis diameter = 5 mm) with lobulated margin in the left internal iliac area (arrow). (c) Fused MR/PET axial image showing slightly increased FDG uptake in the left internal iliac lymph node (arrow). Note slightly increased uptake in the uterine cervical mass (asterisk).

**Table 2 – Accuracy of PET/CT and fused MR/PET in the detection of metastatic lymph node groups in cervical cancer patients.**

| Condition                 | Positive predictive value (95% CI) | Negative predictive value (95% CI) | Sensitivity (95% CI) | Specificity (95% CI) |
|---------------------------|------------------------------------|------------------------------------|----------------------|----------------------|
|                           | %                                  |                                    |                      |                      |
| PET/CT <sup>a</sup>       | 46.4(33.2–60.1)                    | 93.4(90.7–95.3)                    | 44.1(31.4–57.5)      | 93.9(91.3–95.8)      |
| Fused MR/PET <sup>b</sup> | 47.1(35.0–59.5)                    | 94.4(91.9–96.2)                    | 54.2(40.8–67.1)      | 92.7(90.0–94.8)      |

a Image analysis was done with PET/CT only.  
b Image analysis was done with fused MR/PET.

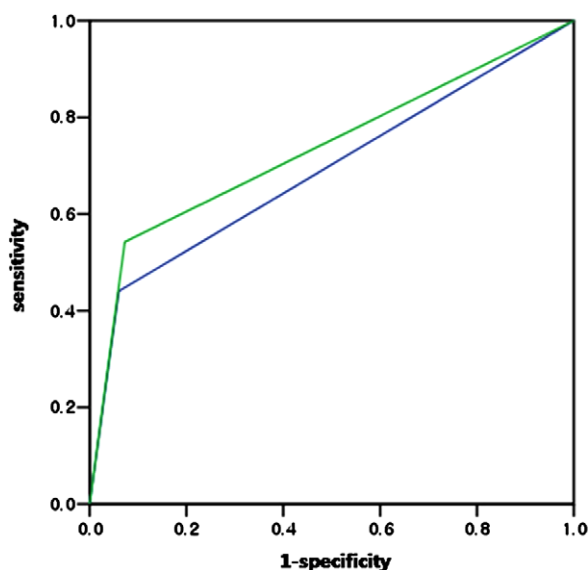


**Fig. 4 – Graphs of ROC analysis results shows additional value of unenhanced images to both readers in detecting lymph node metastases. Blue line, PET/CT images; green line, fused MR/PET images. The areas under the ROC for the PET/CT and fused MR/PET were 0.690 (confidence interval; 0.650–0.728) and 0.735 (0.696–0.771) respectively ( $p = 0.045$ ). (For interpretation of the references to colour in this figure legend, the reader is referred to the web version of this article.)**

FIGO staging of cervical cancer and, accordingly, vigilant preoperative imaging work-up is not usually done.<sup>29</sup>

PET is usually used preoperatively to detect metastatic lymph nodes in patients with uterine cervical cancer; however, there is considerable difficulty in accurately detecting metastatic lymph nodes with this modality. Although PET has clinical advantages with the high lesion-to-background contrast and whole-body data acquisition, making it easy to localise metabolic abnormalities, FDG is not specific for tumour imaging; macrophages involved in inflammatory and infectious diseases can also accumulate in the tracer, and false-negative analysis may result from lymph nodes that are smaller than 1 cm or that contain micrometastases.<sup>18,25</sup> These obstacles are partly attributable to the lower spatial resolution of PET, compared to CT or MRI. The introduction of PET/CT fusion has partly overcome these obstacles.<sup>11</sup> However, the CT images used in the PET/CT fusion are non-contrast images, which can limit adequate detection

of metastatic lymph nodes. In addition, MRI is superior in the characterisation of internal architecture, such as fatty hilum, border of the lymph node, and presence of necrosis, compared to CT. Also, a significant proportion of lymph nodes smaller than 1 cm have a chance of being metastatic ones. Giradi et al.<sup>30</sup> reported that there were micrometastases in 37% of metastatic lymph nodes and Ayhan et al.<sup>31</sup> reported that 56% of metastatic lymph nodes were smaller than 1 cm.

In daily practice, MRI is performed before PET/CT in the work-up of patients with uterine cervical cancer. Therefore, information about the lymph nodes status from the MRI is usually considered in the interpretation of PET/CT. However, the annotated lymph nodes are usually larger than 1 cm; many lymph nodes that are smaller than 1 cm can be identified but are not usually mentioned for further evaluation in MRI, and these small lymph nodes have little chance of being evaluated in PET/CT. Chou et al.<sup>25</sup> reported that PET had little value in early stage cervical cancer patient with small (<1 cm in length) lymph nodes. In our study, the review of fused MR/PET led to the examination of an additional 23 lesions and the detection of six more metastatic nodal groups.

In our study, the surgeons were guided by preoperative MRI and PET/CT and this can cause verification bias. However, in our study we sampled all visible lymph nodes in predetermined lymphatic regions, thus the degree of verification bias was minimised.

In our study, the region specific comparison was also carried out. For this reason the evaluated lymph node could only be the largest lymph node or a lymph node with meaningful findings in the PET/CT scans. For this reason the correlation of all individual lymph nodes with imaging findings could not be fully evaluated. We believe that the node-by-node comparison should be carried out in a future study.

In the present study, we demonstrated that the digital fusion of MRI and PET scans to detect metastatic lymph nodes in cervical cancer patients provided meaningful clinical data. Our information suggests that MRI and PET fusion should be employed in the staging of cervical cancer patients.

In conclusion, our study demonstrated that fused MR/PET imaging of structural and functional data can provide additional diagnostic value in the detection of lymph node metastases in patients with uterine cervical cancer. The addition of MRI offers an increased ability to detect metastatic lymph nodes compared with PET/CT alone. Therefore, we recommend the use of fused MR/PET imaging for the evaluation of lymph node status in patients with uterine cervical cancer.

## Conflict of interest statement

None declared.

## REFERENCES

- Parkin DM, Bray F, Ferlay J, Pisani P. Estimating the world cancer burden: Globocan 2000. *Int J Cancer* 2001;**94**(2):153–6.
- Averette HE, Dudan RC, Ford Jr JH. Exploratory celiotomy for surgical staging of cervical cancer. *Am J Obstet Gynecol* 1972;**113**(8):1090–6.
- Ballon SC, Berman ML, Lagasse LD, Petrilli ES, Castaldo TW. Survival after extraperitoneal pelvic and paraaortic lymphadenectomy and radiation therapy in cervical carcinoma. *Obstet Gynecol* 1981;**57**(1):90–5.
- Takeshima N, Yanoh K, Tabata T, Nagai K, Hirai Y, Hasumi K. Assessment of the revised International Federation of Gynecology and obstetrics staging for early invasive squamous cervical cancer. *Gynecol Oncol* 1999;**74**(2):165–9.
- Tanaka Y, Sawada S, Murata T. Relationship between lymph node metastases and prognosis in patients irradiated postoperatively for carcinoma of the uterine cervix. *Acta Radiol Oncol* 1984;**23**(6):455–9.
- Downey GOR, Adcock LL, Prem KA, Twigg LB. Pretreatment surgical staging in cervical carcinoma: therapeutic efficacy of pelvic lymph node resection. *Am J Obstet Gynecol* 1989;**160**:1055–61.
- Potish RA, Twigg LB, Okagaki T, Prem KA, Adcock LL. Therapeutic implications of the natural history of advanced cervical cancer as defined by pretreatment surgical staging. *Cancer* 1985;**56**(4):956–60.
- Lagasse LD, Creasman WT, Shingleton HM, Ford JH, Blessing JA. Results and complications of operative staging in cervical cancer: experience of the Gynecologic Oncology Group. *Gynecol Oncol* 1980;**9**(1):90–8.
- Chung CK, Nahhas WA, Zaino R, Stryker JA, Mortel R. Histologic grade and lymph node metastasis in squamous cell carcinoma of the cervix. *Gynecol Oncol* 1981;**12**(3):348–54.
- Kupets R, Covens A. Is the International Federation of Gynecology and Obstetrics staging system for cervical carcinoma able to predict survival in patients with cervical carcinoma?: an assessment of clinimetric properties. *Cancer* 2001;**92**(4):796–804.
- Van Nagell Jr JR, Roddick Jr JW, Lowin DM. The staging of cervical cancer: inevitable discrepancies between clinical staging and pathologic findings. *Am J Obstet Gynecol* 1971;**110**(7):973–8.
- Scheidler J, Hricak H, Yu KK, Subak L, Segal MR. Radiological evaluation of lymph node metastases in patients with cervical cancer. A meta-analysis. *Jama* 1997;**278**(13):1096–101.
- Rose PG, Adler LP, Rodriguez M, Faulhaber PF, Abdul-Karim FW, Miraldi F. Positron emission tomography for evaluating para-aortic nodal metastasis in locally advanced cervical cancer before surgical staging: a surgicopathologic study. *J Clin Oncol* 1999;**17**(1):41–5.
- Beyer T, Townsend DW, Brun T, et al. A combined PET/CT scanner for clinical oncology. *J Nucl Med* 2000;**41**(8):1369–79.
- Grigsby PW, Dehdashti F, Siegel BA. FDG-PET Evaluation of Carcinoma of the Cervix. *Clin Positron Imaging* 1999;**2**(2):105–9.
- Narayan K, Hicks RJ, Jobling T, Bernshaw D, McKenzie AF. A comparison of MRI and PET scanning in surgically staged loco-regionally advanced cervical cancer: potential impact on treatment. *Int J Gynecol Cancer* 2001;**11**(4):263–71.
- Reinhardt MJ, Ehrhrt-Braun C, Vogelgesang D, et al. Metastatic lymph nodes in patients with cervical cancer: detection with MR imaging and FDG PET. *Radiology* 2001;**218**(3):776–82.
- Roh JW, Seo SS, Lee S, et al. Role of positron emission tomography in pretreatment lymph node staging of uterine cervical cancer: a prospective surgicopathologic correlation study. *Eur J Cancer* 2005;**41**(14):2086–92.
- Sugawara Y, Eisbruch A, Kosuda S, Recker BE, Kison PV, Wahl RL. Evaluation of FDG PET in patients with cervical cancer. *J Nucl Med* 1999;**40**(7):1125–31.
- Schoder H, Yeung HW, Gonen M, Kraus D, Larson SM. Head and neck cancer: clinical usefulness and accuracy of PET/CT image fusion. *Radiology* 2004;**231**(1):65–72.
- Cerfolio RJ, Ojha B, Bryant AS, Raghuveer V, Mountz JM, Bartolucci AA. The accuracy of integrated PET-CT compared with dedicated PET alone for the staging of patients with nonsmall cell lung cancer. *Ann Thorac Surg* 2004;**78**(3):1017–23. discussion 1017–23.
- Martinelli M, Townsend D, Meltzer C, Villemagne VV. 7. Survey of results of whole body imaging using the PET/CT at the University of Pittsburgh Medical Center PET facility. *Clin Positron Imaging* 2000;**3**(4):161.
- Lardinois D, Weder W, Hany TF, et al. Staging of non-small-cell lung cancer with integrated positron-emission tomography and computed tomography. *N Engl J Med* 2003;**348**(25):2500–7.
- Aquino SL, Asmuth JC, Alpert NM, Halpern EF, Fischman AJ. Improved radiologic staging of lung cancer with 2-18F-fluoro-2-deoxy-D-glucose-positron emission tomography and computed tomography registration. *J Comput Assist Tomogr* 2003;**27**(4):479–84.
- Chou HH, Chang TC, Yen TC, et al. Low value of 18F-fluoro-2-deoxy-D-glucose positron emission tomography in primary staging of early-stage cervical cancer before radical hysterectomy. *J Clin Oncol* 2006;**24**(1):123–8.
- Ma SY, See LC, Lai CH, et al. Delayed (18)F-FDG PET for detection of paraaortic lymph node metastases in cervical cancer patients. *J Nucl Med* 2003;**44**(11):1775–83.
- Choi HJ, Kim SH, Seo SS, et al. MRI for pretreatment lymph node staging in uterine cervical cancer. *AJR Am J Roentgenol* 2006;**187**(5):W538–43.
- Lanciano RM, Corn BW. The Role of surgical staging for cervical cancer. *Semin Radiat Oncol* 1994;**4**(1):46–51.
- Kamura T, Tsukamoto N, Tsuruchi N, et al. Multivariate analysis of the histopathologic prognostic factors of cervical cancer in patients undergoing radical hysterectomy. *Cancer* 1992;**69**(1):181–6.
- Girardi F, Petru E, Heydarfadaei M, Haas J, Winter R. Pelvic lymphadenectomy in the surgical treatment of endometrial cancer. *Gynecol Oncol* 1993;**49**(2):177–80.
- Ayhan A, Tuncer ZS, Tuncer R, Yuce K, Kucukali T. Tumor status of lymph nodes in early endometrial cancer in relation to lymph node size. *Eur J Obstet Gynecol Reprod Biol* 1995;**60**(1):61–3.